Distance-adaptive, Low CAPEX Cost p-Cycle Design Without Candidate Cycle Enumeration in Mixed-Line-Rate Optical Networks

Min Ju, *Student Member, IEEE*, Fen Zhou, Zuqing Zhu, *Senior Member, IEEE*, and Shilin Xiao

***Abstract*—Even though elastic optical networks (EONs) are promising to provision increasingly dynamic and heterogeneous traffic, the requirements on bandwidth-variable optical devices bring upgrading challenges in current wavelength-division multiplexing (WDM) optical networks. Mixed-line-rate (MLR) optical networks offer a transitional solution that allows several coexisting line rates (e.g., $10/40/100$ Gb/s). In this paper, we investigate distance-adaptive preconfigured-cycle (p-Cycle) protection scheme in MLR optical networks. Path-length-limited p-cycles are designed to be assigned line rate depending on the length of each protection path. Instead of conventional candidate cycle enumeration, a mixed integer linear programming (MILP) model is formulated to directly generate the optimal p-cycles with the minimum capital expenditures (CAPEX) cost. We also develop two algorithms to make the proposed MILP model scalable. Simulation results indicate that the algorithms are time efficient for solving the MILP-based p-cycle design. We further compare our p-cycle design method with other schemes, and demonstrate that our method largely reduces the CAPEX cost for more than 40%, mainly in transponder cost. To the best of our knowledge, this is the first time that distance-adaptive p-cycle design without candidate cycle enumeration is proposed for MLR optical networks.**

***Index Terms*—Distance-adaptive, mixed line rates (MLR) optical networks, mixed integer linear programming (MILP), preconfigured-cycle (p-cycle).**

I. Introduction

TRAFFIC demands in today's backbone optical networks are becoming increasingly dynamic and heterogeneous due to high-bandwidth applications, i.e., commercial data-center backhaul, cloud computing and distributed storage. Elastic optical networks (EONs) are regarded as the promising solution to provision such traffic with flexible spectrum allocation [1]–[3]. However, the requirements on bandwidth-variable transponders (BVTs) and bandwidth-variable optical cross-connects (BV-OXCs) are the main challenges of upgrading current wavelength division multiplexing (WDM) optical networks to EONs. Meanwhile, mixed-line-rate (MLR) optical networks with coexisting line rates ($10/40/100$ Gb/s) can be the transitional solution, which has been proved to achieve the comparable performance as EONs [4]. In MLR optical networks, different types of transponders are configured to provision traffic at several line rates [5]–[7]. Line rate assignment should consider the transponder cost as well as transmission reach limits. Hence, appropriate line rates should be assigned to efficiently allocate network resources in MLR optical networks.

As it is demonstrated that a single optical fiber can carry over 20 Tb/s traffic transmission capacity, a failure in an MLR network element (e.g., a fiber cut) can cause huge data loss [8]. Previously, survivable WDM optical networks have been investigated intensively with several protection schemes [9]–[13]. However, these protection schemes only focus on network resources allocation under single line rate (SLR). Survivability in MLR optical networks needs to deal with line rate assignment related to protection cost and transmission reach. Thus, cost-effective protection approaches for MLR optical networks are increasingly important.

Pre-configured-cycle (p-Cycle) strategy has fast switching speed, and it provides protection capacity for both on-cycle links and straddling links [14]. Specifically, the protection capacity of p-cycle is configured in advance, only the two ending nodes of the failed link switch the working traffic to pre-configured protection path. More importantly, one unit of protection capacity is provided for each on-cycle link in one p-cycle, while two units of protection capacity are provided for each straddling link. p-Cycle protection scheme is very attractive owing to these advantages in optical network protection.

Conventional p-cycle design schemes are required to enumerate candidate cycle set in advance, and to screen p-cycles from the candidate cycle set. Since the number of candidate cycles increases exponentially with the number of nodes and links in the network, it would be intractable to enumerate all the candidate cycles. Thus, some work on finding partial candidate cycles with high metric have tried to form effective

Manuscript received November 6, 2015; revised February 15, 2016 and March 29, 2016; accepted March 29, 2016. Date of publication March 31, 2016; date of current version April 30, 2016. This work was supported in part by the Open Project Program (2013GZKF031309) of the State Key Laboratory of Advanced Optical Communication Systems and Networks in China, National Nature Science Fund of China under Grants 61271216, 61221001, 61090393, and 61433009, National "863" Hi-tech Project of China under Grants 2013AA013602 and 2012AA011301, and China Scholarship Council ([2015]3022).

M. Ju is with the State Key Laboratory of Advanced Optical Communication Systems and Networks, Shanghai Jiao Tong University, Shanghai 200240, China. She is also with the Computer Science Laboratory, University of Avignon, Avignon 84000, France (e-mail: min.ju@alumni.univ-avignon.fr).

F. Zhou is with the Computer Science Laboratory, University of Avignon, Avignon 84000, France (e-mail: fen.zhou@univ-avignon.fr).

Z. Zhu is with the School of Information Science and Technology, University of Science and Technology of China, Hefei 230027, China (e-mail: zqzhu@ieee.org).

S. Xiao is with the State Key Laboratory of Advanced Optical Communication Systems and Networks, Shanghai Jiao Tong University, Shanghai 200240, China (e-mail: slxiao@sjtu.edu.cn).

Color versions of one or more of the figures in this paper are available online at http://ieeexplore.ieee.org.

Digital Object Identifier 10.1109/JLT.2016.2549642

candidate cycle sets, nevertheless, optimal solution cannot be obtained with them. In addition, p-cycles without candidate cycle enumeration are explored in [12]–[15], but these methods are not valid in MLR optical networks due to the lack of line rate optimization. Moreover, p-cycles are rarely designed considering transmission reach limits, which is not realistic.

In this paper, we extend our work in [16] and further investigate distance-adaptive p-cycle protection without candidate cycle enumeration in MLR optical networks. Path-length-limited p-cycles are designed to assign line rates depending on the length of each protection path. We formulate a mixed integer linear programming (MILP) model to minimize CAPEX cost. Then, we propose graph partitioning in average (GPA) algorithm and Estimation of cycle numbers $|I|$ (EI) algorithm to enable concurrent computation in sub-graphs with the proposed MILP model. These two algorithms are proved to be efficient, and it is also demonstrated that our p-cycle design achieves significant CAPEX cost savings in comparison to p-cycle design with SLR and p-cycle design with candidate cycle enumeration. To the best of our knowledge, this is the first time that p-cycle protection design without candidate cycle enumeration is proposed for MLR optical networks. The key contributions of this paper are summarized as follows:

1) Distance-adaptive p-cycle are designed in the consideration of transmission reach at various line rates, thus the transmission quality of optical signal along protection path can be guaranteed.
2) An MILP model without candidate cycle enumeration is formulated to directly generate p-cycles, thus it is guaranteed to obtain the optimal solution if possible.
3) p-Cycles are generated with the path-length-limited constraint, which restricts p-cycles according to the length of each protection path instead of the length of cycle circumference. It is more accurate and cost-effective.
4) Graph partitioning algorithm is developed to enable concurrent computation in sub-graphs in the proposed MILP model, which largely reduces computing time.

The rest of this paper is organized as follows. Related work is reviewed in Section II. Section III describes the p-cycle protection problem in MLR optical networks. We study p-cycle design without candidate cycle enumeration and formulate an MILP model in Section IV. Thereafter, in Section V, we develop two algorithms to solve the MILP model time-efficiently. The performance of our p-cycle design is evaluated in Section VI. Finally, we conclude the paper in Section VII.

II. Related Work

Even though survivable MLR optical networks are critical, very few related work has been done in this field [6], [17]–[19]. In [6], three dedicated protection approaches at the lightpath level were studied in MLR networks. The authors further explored shared subconnection protection in transparent MLR networks in [18], in which they designed a two-step approach to solving the routing/rate assignment and wavelength assignment. Vadrevu *et al.* [19] investigated survivable provisioning with multipath routing to minimize overall transponder cost, in which partial requested bandwidth was provisioned on link-disjoint path. However, these protection schemes mainly focused on end-to-end path protection, thus they may suffer from relatively long restoration time since the working and protection paths had to be set up and turn down frequently.

p-Cycle protection scheme with fast switching time was introduced in 1998 [14]. In [20], link-based p-cycles were explored to protect individual links with and without wavelength conversion. p-Cycle was also developed to protect shared risk link group failure in [21], and to provide protection for links and nodes failures simultaneously [22]. In addition, Akpuh and Doucette [23] developed a new integer linear programming (ILP) model for enhanced failure-specific p-cycles with a specified minimum dual-failure restorability level. They showed that this new model provided significant capacity cost reductions compared with the original design model, which did not consider this enhanced dual-failure restorability. Moreover, Cholda and Jajszczyk [24] addressed the impact on reliability performance of p-cycles due to capacity sharing, and they concluded that there was a tradeoff between capacity sharing and reliability. For the reliability concern, they obtained that it is more reasonable to use p-cycles in smaller networks than in long haul networks.

All the p-cycle protection schemes above with SLR used a two-step approach to enumerating candidate cycles first, and then to screen p-cycles from the candidate cycles. However, enumerating all the candidate cycles would increase the computational complexity since the number of candidate cycles increases exponentially with the number of network links and nodes. Akpuh and Doucette [25] comprehensively analyzed the tradeoff among the size of eligible p-cycles, the optimality gap and computing time. To ensure a small enough optimality gap, a bigger eligible set of p-cycles needed to be selected, thus long computing time was also required. To address this issue, some heuristic algorithms for enumerating partial candidate cycles with high metric were proposed [26] [27]. Even though these partial candidate cycles were individually efficient, they generally provided only sub-optimal solutions when combined together. A single-step method using column generation technique was proposed to reach optimal solution and own scalability in [28], but it relied on a decomposition of the initial problem into master problem and pricing problem.

p-Cycle design without candidate cycle enumeration was studied by ILP formulations in [12], however, the ILP was too complex so that a four-step heuristic was proposed to solve it. The authors further designed three efficient p-cycle design without candidate cycle enumeration for SLR optical networks in [15], which were based on recursion, flow conservation, and cycle exclusion, respectively. However, these optimal p-cycle design approaches without candidate cycle enumeration were only valid in SLR optical networks, and they cannot be applied into MLR optical networks due to the lack of line rate optimization. More importantly, the transmission reach was ignored in their models, thus it cannot guarantee the transmission quality along the protection path.

Even though a p-cycle design was investigated for MLR optical networks in [17], it still required candidate cycle

enumeration in advance and screened p-cycles from candidate cycle set. More importantly, Drid *et al.* [17] did not consider various transparent transmission reaches at different line rates, thus the quality of the optical signal on the protection path cannot be guaranteed.

Hence, it is of great value to investigate distance-adaptive p-cycle design scheme without candidate cycle numeration in MLR optical networks.

III. Distance-Adaptive p-Cycle Protection for MLR Optical Networks

In this section, we first explain the principle of distance-adaptive p-cycle design for MLR optical networks. Thereafter, an example is given to show distance-adaptive p-cycle design with minimum CAPEX cost.

The MLR optical network topology is modeled as $G(V, E)$, where V and E represent the sets of nodes and directed fiber links in G, respectively. A set of line rates, denoted by $R = 10/40/100$ Gb/s, is assumed to provision the traffic loads. p-Cycles are built to provide protection for single link failure under the transmission reach limits. We assume that the protection paths are provisioned in transparent optical networks without any optical-electrical-optical (O/E/O) conversion in intermediate node(s), then only two transponders at the ending nodes are laid for each protection path. Thus, contiguous line rate should be guaranteed along the protection paths. The distance-adaptive p-cycles for MLR optical networks in this study are designed under the following considerations:

1) *Transmission reach limits*: The quality of an optical signal is degraded along a path due to physical-layer impairments [29], and it becomes even worse in MLR optical networks with various co-existing line rates. The maximum transmission reaches of line rates at 10, 40, and 100 Gb/s are 1750, 1800, and 900 km at a threshold bit-error-rate 10^{-3}, respectively [5]. The transmission reach in [5] was estimated with modulation formats of 10 Gb/s OOK, 40 Gb/s DPSK and 100 Gb/s DP-QPSK. Moreover, the MLR optical networks was considered dispersion minimized for 10 Gb/s (as in legacy systems). Transmission reach limit is a main consideration to determine the proper line rate for each p-cycle. As shown in Fig. 1, the protection path $a-b-c-d$ for failed link $a-d$ has a length of 1780 km, then only 40 Gb/s can be assigned.
2) *Transponders Cost*: The relative transponder cost is treated as 1, 2.5 and 3.75 units for 10, 40 and 100 Gb/s, respectively [5].
3) *Spare Capacity Cost*: Spare capacity is required for each link on the p-cycles. We treat the spare capacity cost as 1 for each link. Transponder cost and spare capacity cost are considered together as the CAPEX cost in this study.
4) *SLR for One p-Cycle*: Only one SLR can be selected for one p-cycle, even though several line rates are potential for individual protection path in the p-cycle. Again in Fig. 1, protection path $d-a-b-c$ with 1600 km length for failed link $d-c$ can be assigned 10 or 40 Gb/s, but only 40 Gb/s is allowable because another protection path $a-b-c-d$ with 1780 km length only can be assigned 40 Gb/s.
5) *p-Cycle Protection Capacity*: One unit of protection capacity is provided for each on-cycle link, while for each straddling link, two units of protection capacity are provided. For the on-cycle link $a-d$ in Fig. 1, the p-cycle provides 40 Gb/s protection capacity, while it provides 2×40 Gb/s $= 80$ Gb/s protection capacity for straddling link $a-c$. The protection capacity provided by all p-cycles should be sufficient to ensure 100% single link failure protection.

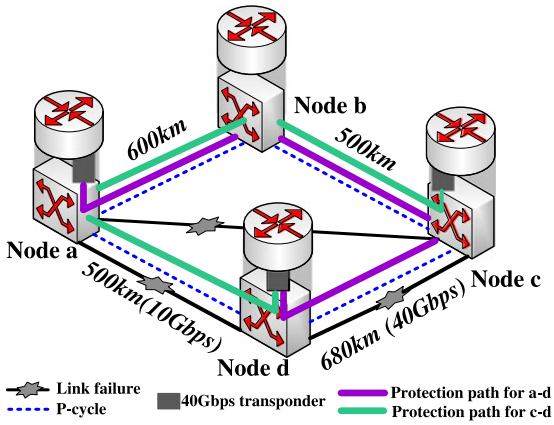

Fig. 1. p-Cycle protection in MLR optical networks.

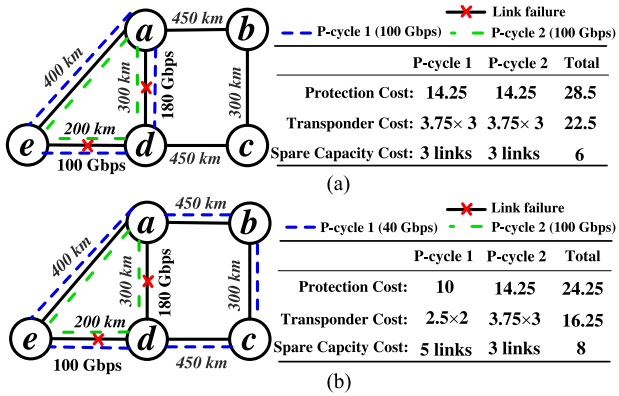

Fig. 2. Optimal p-cycle design with the minimum CAPEX cost. (a) Feasible solution of p-cycles. (b) Optimal solution of p-cycles.

Hence, MLR optical networks offer the potential to optimize line rates of p-cycles with respect to traffic amount, transmission reach limits, CAPEX cost and protection capacity. However, conventional p-cycle design with MLR only consider transponder cost, spare capacity cost and protection capacity. In our work, we further take into account the transmission reach limits and explore accurate line rate assignment for distance-adaptive p-cycle design for MLR optical networks.

Here, a simple example in Fig. 2 shows how we design distance-adaptive p-cycle with minimum CAPEX cost. The value next to each link indicates the physical length and the other value on links $a-d$, $e-d$ show the working traffic amount. To protect these two working links, several solutions can be

performed under the previous considerations. Fig. 2(a) shows one feasible solution, where two p-cycles are designed and each of them is assigned 100 Gb/s line rate, thus the CAPEX cost for protection is 28.5. However, CAPEX cost can be further minimized with optimal line rate assignment. Fig. 2(b) shows the optimal p-cycle design with CAPEX cost 24.25, in which p-cycle 1 and p-cycle 2 are assigned with 40 and 100 Gb/s line rates, respectively. Thus, it saves 15% CAPEX cost than that in Fig. 2(b).

IV. MILP Formulation for p-Cycle Design Without Candidate Cycle Enumeration

In this section, we introduce the distance-adaptive p-cycle design for MLR optical networks. Specifically, instead of candidate cycle enumeration, we formulate an MILP model to generate optimal p-cycles with respect to line rate assignment, transmission reach limits, transponder cost and spare capacity cost. We further explore path-length-limited p-cycles to assign line rates depending on the length of each protection path. The inputs and variables in the MILP model are given as follows.

A. MILP Model

$Parameters$:

1) I: The set with the maximum number of p-cycles allowed in the MILP model. The size of I is estimated by (31) in Section V-B.
2) i: Cycle index where $i \in \{1, 2, \ldots, |I|\}$. I_i indicates the ith p-cycle.
3) $G(V, E)$: Network topology with node set V and link set E.
4) N_v: The neighborhood of a node v.
5) d_{vu}: The length between node v and node u, $d_{\max}$ indicates the biggest length in network $G(V, E)$.
6) $r \in R$: The set of line rates, e.g., $\{10, 40, 100$ Gb/s$\}$.
7) h_r: Maximum transmission reach at line rate r, which is 1750, 1800 and 900 km at 10, 40 and 100 Gb/s, respectively. $h_{\max}$ and $h_{\min}$ separately represent the maximum and minimum transmission reach among these three line rates, i.e., $h_{\max}$=1800 km, and $h_{\min}$=900 km.
8) t_r: Transponder cost at line rate r, which is 1, 2.5, and 3.75 at 10, 40 and 100 Gb/s, respectively.
9) c_{vu}: The cost of adding one unit of spare capacity to link (v, u), which is treated as 1 for each link.
10) l_{vu}: Traffic load on undirected link (v, u). As we protect undirected links, only upper triangular matrix in the traffic matrix is valid.

$Variables$:

1) x^i_{vu}: Equals 1 if link (v, u) is used by I_i, otherwise 0.
2) y^i_v: Equals 1 if node v is crossed by I_i, otherwise 0.
3) f^i_v: Virtual $voltage$ value of node v in I_i, $f^i_v \in (0, 1)$.
4) o^i_v: Equals 1 if node v is root node in I_i, otherwise 0.
5) b^i_r: Equals 1 if I_i operates at line rate r, otherwise 0.
6) z^i_{vu}: Equals 1 if link (v, u) is potential to be protected by I_i, otherwise 0.
7) q^i_{vu}: Equals 1 if link (v, u) desires to be protected by I_i, otherwise 0.
8) $q^{\mathrm{ir}}_{\mathrm{vu}}$: Equals 1 if link (v, u) desires to be protected by I_i at line rate r, otherwise 0.
9) y^{ir}_v: Equals 1 if node v is crossed by I_i at line rate r, otherwise 0.
10) $p^{\mathrm{ir}}_{\mathrm{vu}}$: Protection capacity for link (v, u) if it desires to be protected by I_i at line rate r. It equals 1 if link (v, u) is an on-cycle link, and it equals 2 if link (v, u) is straddling link, otherwise 0.

For the sake of readability, we use $\forall i$, $\forall v$, $\forall u$, $\forall r$, and $\forall a$ to denote $\forall i \in \{1, 2, \ldots, |I|\}$ $\forall v \in V$, $\forall u \in N_v$, $\forall r \in R$, and $\forall a \in E$, respectively.

$Objective$:

The objective of our p-cycle design is to minimize the total CAPEX cost consisting of transponder cost and spare capacity cost in MLR optical networks protection. It should be noted in our p-cycle design, only one transponder is laid in one node if there exists at least a protection path incident to this node. It is more cost-effective compared with the conventional p-cycle design in which two transponders are laid at two ending nodes of each protection path, respectively.

$$\begin{aligned} \min \quad & \beta \cdot C_T + \theta \cdot C_L \\ & C_T = \sum_{i \in I} \sum_{r \in R} \sum_{v \in V} t_r \cdot y^{\mathrm{ir}}_v \\ & C_L = \sum_{i \in I} \sum_{a \in E} c_a \cdot x^i_a \end{aligned} \tag{1}$$

where C_T is total transponder cost, and C_L is total spare capacity. β and θ are adjustable parameters for weighting of these two metrics. In this study, we regard both of them as 1.

$Constraints$:

The constraints in MILP model can be classifies into cycle generation constraints (2)–(6), line rate assignment constraints (7), (8) and protection capacity constraints (9)–(15).

1) Cycle Generation Constraints:

$$x^i_{\mathrm{vu}} + x^i_{\mathrm{uv}} \le 1 \quad \forall i, \forall v, \forall u \tag{2}$$

$$\sum_{u \in N_v} (x^i_{\mathrm{vu}} + x^i_{\mathrm{uv}}) = 2y^i_v \quad \forall i, \forall v \tag{3}$$

$$f^i_u - f^i_v \ge (1 + \alpha) x^i_{\mathrm{vu}} - 1 \quad \forall i, \forall v, \forall u \tag{4}$$

$$\sum_{v \in V} o^i_v \le 1 \quad \forall i \tag{5}$$

$$\sum_{u \in N_v} x^i_{\mathrm{vu}} \le 1 + o^i_v \quad \forall i, \forall v. \tag{6}$$

It should be noted that we design undirected p-cycles that protect undirected traffic, but directed links are used in the constraints (2)–(6) in order to generate cycles easily from the formulation.

Constraint (2) ensures that at most one link between two nodes can be used in a p-cycle. Constraint (3) implies that if node v is crossed by a p-cycle, then it should have two adjacent links. In order to guarantee that only one single cycle is generated, we further formulate constraint (4)–(6) to eliminate other cycles with $voltage$ conflict and make sure the generated cycle is a

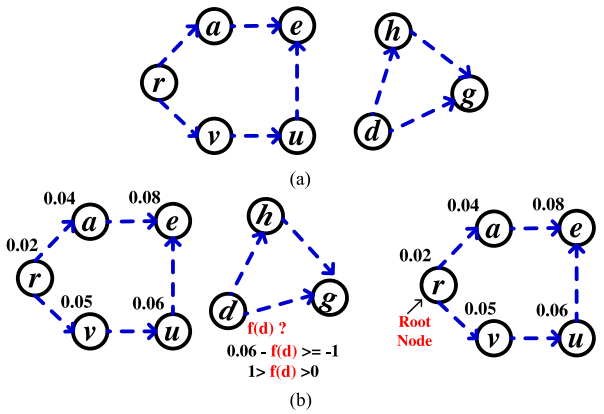

Fig. 3. Cycle generation with and without "$voltage$." (a) Invalid p-cycle generation without "voltage." (b) Voltage conflict. (c) Valid p-cycle generation with "voltage."

connected graph, as shown in Fig. 3. Here, $voltage$ is a virtual variable that is only used to generate single cycle. Constraint (4) ensures that node u should have a bigger $voltage$ than node v if link (v,u) is used in a p-cycle. Constraint (5) ensures there exists only one root node in a p-cycle. Meanwhile, constraint (6) guarantees that only the root node in a p-cycle has two outgoing links.

These constraints guarantee that one single p-cycle is generated and it is a connected graph.

2) Line Rate Assignment Constraints:

$$\frac{\sum_{a\in E} d_a \cdot x_a^i}{h_r} \le \frac{h_{\max}}{h_{\min}} \cdot (1 - b_r^i) + b_r^i, \quad \forall i, \forall r, \forall a \tag{7}$$

$$\sum_{r\in R} b_r^i \le 1 \quad \forall i. \tag{8}$$

Constraint (7) permits to assign line rate for distance-adaptive p-cycles. Specifically, the p-cycle circumference should be less than the transmission reach h_r of the assigned line rate r. We call constraint (7) the cycle-circumference-limited constraint. Note that we assume that the impairments along the protection path are mainly due to long-distance transmission, and the impairments introduced by the intermediate nodes are relatively small so that they can be compensated with a performance margin preset [3]. Constraint (8) ensures that only one line rate can be assigned for each p-cycle.

These constraints guarantee one proper line rate for each p-cycle.

3) Protection Capacity Constraints:

$$z_{\mathrm{vu}}^i \le \frac{1}{2} \cdot (y_v^i + y_u^i), \quad \forall i, \forall v, \forall u \tag{9}$$

$$q_{\mathrm{vu}}^i \le z_{\mathrm{vu}}^i, \quad \forall i, \forall v, \forall u, u > v \tag{10}$$

$$q_{\mathrm{vu}}^{\mathrm{ir}} = q_{\mathrm{vu}}^i \cdot b_r^i, \quad \forall i, \forall r, \forall v, \forall u, u > v \tag{11}$$

$$p_{\mathrm{vu}}^{\mathrm{ir}} = (2 \cdot z_{\mathrm{vu}}^i - x_{\mathrm{vu}}^i - x_{\mathrm{uv}}^i) \cdot q_{\mathrm{vu}}^i \cdot b_r^i \quad \forall i, \forall r, \forall v, \forall u, u > v \tag{12}$$

$$\sum_{i\in I} \sum_{r\in R} p_{\mathrm{vu}}^{\mathrm{ir}} \cdot r \ge l_{\mathrm{vu}}, \quad \forall v, \forall u, u > v \tag{13}$$

$$y_v^{\mathrm{ir}} \ge q_{\mathrm{vu}}^{\mathrm{ir}}, \quad \forall i, \forall r, \forall v, \forall u, u > v \tag{14}$$

$$y_u^{\mathrm{ir}} \ge q_{\mathrm{vu}}^{\mathrm{ir}}, \quad \forall i, \forall r, \forall v, \forall u, u > v. \tag{15}$$

TABLE I
COMPUTATIONAL COMPLEXITY OF THE MILP MODEL

Variables	Number
$x_{\mathrm{uv}}^i, z_{\mathrm{uv}}^i, q_{\mathrm{uv}}^i$	$3\|I\| \times \|E\|$
y_v^i, o_v^i, f_v^i	$3\|I\| \times \|V\|$
b_r^i	$\|I\| \times \|R\|$
$q_{\mathrm{uv}}^{\mathrm{ir}}, p_{\mathrm{uv}}^{\mathrm{ir}}$	$2\|I\| \times \|E\| \times \|R\|$
y_v^{ir}	$\|I\| \times \|V\| \times \|R\|$
Constraints	**Number**
(2)–(6)	$2\|I\| \times \|E\| + 2\|I\| \times \|V\| + \|I\|$
(7)–(8)	$\|I\| \times \|E\| \times \|R\| + \|I\|$
(9)–(10) and (13)–(17)	$\frac{3}{2}\|I\| \times \|E\| + \frac{7}{2}\|I\| \times \|E\| \times \|R\| + \frac{1}{2}\|E\|$

We give a limitation of the directed links used in the protection capacity constraints to guarantee the protection capacity for undirected traffic. Specifically, only the link (v,u) with u bigger than v is considered to be provided protection.

Constraint (9) makes sure that only if both starting and ending nodes of a link (v,u) are crossed by I_i, then link (v,u) is potential to be protected by I_i. Constraint (10) implies the desire of link (v,u) to be protected by one p-cycle. Constraint (11) determines that if link (v,u) desires to be protected by I_i at line rate r. Constraint (12) determines the protection capacity for link (v,u) if it desires to be protected by I_i. Specifically, if link (v,u) is an on-cycle link, one protection capacity is provided, else if it is a straddling link, two protection capacity units are provided, otherwise, no protection capacity is provided. Constraint (13) ensures 100% single link failure protection. Constraints (14) and (15) ensure that one transponder at line rate r should be laid on node v in I_i if at least one link incident to v desires to be protected by this I_i at line rate r.

These constraints ensure enough protection capacity for undirected traffic by the p-cycles. In order to ensure linearity in the MILP model, constraints (11) and (12) are rewritten as constraints

$$\Longrightarrow \begin{cases} q_{\mathrm{vu}}^{\mathrm{ir}} \le \frac{1}{2} \cdot (q_{\mathrm{vu}}^i + b_r^i), & \forall i, \forall r, \forall v, \forall u, u > v \\ q_{\mathrm{vu}}^{\mathrm{ir}} \ge q_{\mathrm{vu}}^i + b_r^i - 1, & \forall i, \forall r, \forall v, \forall u, u > v \end{cases} \tag{16}$$

$$\Longrightarrow \begin{cases} p_{\mathrm{vu}}^{\mathrm{ir}} \le 2 \cdot q_{\mathrm{vu}}^i, & \forall i, \forall r, \forall v, \forall u, u > v \\ p_{\mathrm{vu}}^{\mathrm{ir}} \le 2 \cdot b_r^i, & \forall i, \forall r, \forall v, \forall u, u > v \\ p_{\mathrm{vu}}^{\mathrm{ir}} \le 2 \cdot z_{\mathrm{vu}}^i - x_{\mathrm{vu}}^i - x_{\mathrm{uv}}^i, & \forall i, \forall r, \forall v, \forall u, u > v. \end{cases} \tag{17}$$

B. Computational Complexity

The variables and constraints of the MILP model are summarized in Table I. The total number of variables and constraints are $|I|\times(9|E|+6|V|+3)$ and $|I|\times(16|E|+2|V|+2)+\frac{1}{2}|E|$, respectively (*we assign* $|R|=3$ *as we have three line rates*). Both of variables and constraints only increase linearly with the network size if $|I|$ is given.

C. Path-Length-Limited p-Cycle

In Section IV-A, we use simple and faster cycle-circumference-limited constraint (7) to assign line rate with transmission reach limits. In fact, both hop-limited

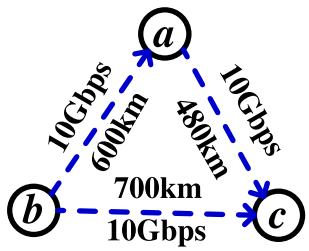

P-cycle generation with constraint (7)	
Line Rate:	40Gbps
Protection Cost:	10.5
Transponder Cost:	2.5×3nodes
Spare Capacity Cost:	3 links
P-cycle generation with constraint (20)	
Line Rate:	10Gbps
Protection Cost:	6
Transponder Cost:	1×3nodes
Spare Capacity Cost:	3 links

Fig. 4. Extra CAPEX cost in p-cycle using constraint (7).

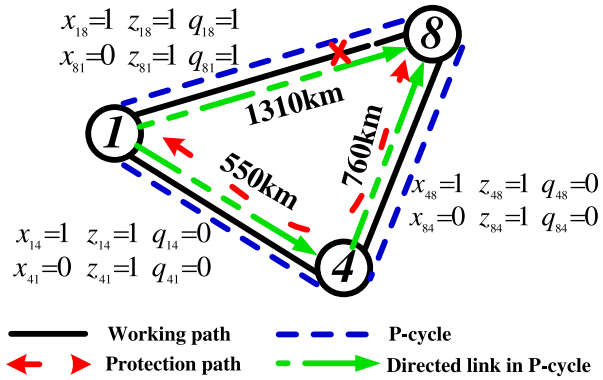

Fig. 5. The feasible solution is eliminated by cycle-circumference-limited constraint (7). We show the value of variables x^i_{vu}, z^i_{vu} and q^i_{vu} in the feasible solution with path-length-limited p-cycle.

and cycle-circumferences-limited constraints have been tried in [30]–[32]. In these studies, hop-limited p-cycle design excluded p-cycle directly with maximum H hops of any protection path, while cycle-circumferences-limited design restricted p-cycle with the maximum $H+1$ hops of the cycle circumference. They obtained the conclusion that simple and faster cycle-circumference-limited model provided an excellent approximation of the strictly hop-limited model. However, considering the transmission reach limits in MLR optical networks, cycle-circumference-limited constraint in p-cycle design will result in extra CAPEX cost and even infeasible solution as follows.

1) *Extra CAPEX cost*: For instance in Fig. 4, all the links with traffic 10 Gb/s need to be protected. The p-cycle is assigned 40 Gb/s line rate by using constraint (7) as the length of the p-cycle circumference is 1780 km. Thus, the CAPEX cost is 10.5. However, if the line rate assignment depends on the length of each protection path, which are $a-b-c$ (1300 km), $a-c-b$ (1180 km) and $b-a-c$ (1080 km), thus 10 Gb/s line rate can be assigned with a smaller CAPEX cost of 6. We call p-cycle with such line rate constraint *path-length-limited p-cycle*.
1) *Infeasible solution*: More importantly, in some cases, the cycle-circumference-limited constraint (7) results in infeasible solution even though there exists a feasible solution. For instance, constraint (7) will eliminate the p-cycle in Fig. 5 as its cycle circumference length 2620 km is bigger than the maximum transmission reach (1800 km at 40 Gb/s). Note that such p-cycle design with cycle-circumference-limited constraint also exists in [13]–[33], in which the length of p-cycle circumference is used as transmission reach to determine line rate or modulation format. In fact, the p-cycle in Fig. 5 still enables the protection for link 1–8 using protection path $1-4-8$, as the protection path length is only 1310 km, which is able to be assigned 10 or 40 Gb/s line rate.

We propose the following theorems to address path-length-limited p-cycle with transmission reach limits on each protection path.

Theorem 1: A cycle (say I_i) is a path-length-limited p-cycle if the following two conditions are held:

$$z^i_b = q^i_b = 1, \quad \exists \quad b \in E \tag{18}$$

$$\sum_{a\in E} d_a \cdot x^i_a - d_b \le h_r, \quad \exists \quad r. \tag{19}$$

Proof: Equation (18) indicates that at least one link b can be protected by I_i and it also desires to be protected by I_i. In inequality (19), $\sum_{a\in E} d_a \cdot x^i_a$ calculates the length of cycle circumference of I_i, which consists of all the on-cycle links. Then, the length of protection path for link b in I_i depends on the nature of link b:

1) *On-cycle link*: $\sum_{a\in E} d_a \cdot x^i_a - d_b$ represents the protection path length for link b. Obviously, if it is less than h_r, then at least one line rate r can be assigned for I_i.
2) *Straddling link*: There are two protection paths for link b: $v-u_1-\cdots-u_n-u$ and $v-v_1-\cdots-v_n-u$ (here, u_i and v_i indicate the intermediate nodes along the protection path). Thus the corresponding lengths of these two protection paths are $D^1_{\mathrm{vu}} = d_{\mathrm{vu}_1} + d_{u_1u_2} + \cdots + d_{u_n u}$ and $D^2_{\mathrm{vu}} = d_{\mathrm{vv}_1} + d_{v_1v_2} + \cdots + d_{v_n u}$, respectively, and they should satisfy $D^1_{\mathrm{vu}} + D^2_{\mathrm{vu}} = \sum_{(v,u)\in E} d_{\mathrm{vu}} \cdot x^i_{\mathrm{vu}}$. According to the triangle inequality, it is obvious that $d_{\mathrm{vu}} \le D^1_{\mathrm{vu}}, D^2_{\mathrm{vu}}$. Then, $\sum_{(v,u)\in E} d_{\mathrm{vu}} \cdot x^i_{\mathrm{vu}} - d_{\mathrm{vu}} \ge \sum_{(v,u)\in E} d_{\mathrm{vu}} \cdot x^i_{\mathrm{vu}} - D^1_{\mathrm{vu}}$, $\sum_{(v,u)\in E} d_{\mathrm{vu}} \cdot x^i_{\mathrm{vu}} - d_{\mathrm{vu}} \ge \sum_{(v,u)\in E} d_{\mathrm{vu}} \cdot x^i_{\mathrm{vu}} - D^2_{\mathrm{vu}}$. Thus, if inequality (19) is held, then the two protection paths of b in I_i can at least operate at line rate r.

Hence, I_i is a path-length-limited p-cycle if conditions (18) and (19) are held. ■

Theorem 2: A path-length-limited p-cycle can be found by constraint (20) if it exists, and its appropriate line rate can also be determined by

$$\frac{\sum_{a\in E} d_a \cdot x^i_a - q^i_{\mathrm{vu}} \cdot d_{\mathrm{vu}}}{h_r} \le \frac{h_{\max}}{h_{\min}} \cdot (1 - b^i_r) + b^i_r + \frac{d_{\max}}{h_r} \cdot (1 - q^i_{\mathrm{vu}}), \quad \forall i, \forall r, \forall v, \forall u, u > v. \tag{20}$$

Proof: In constraint (20), x^i_{vu} represents whether link (v,u) is used as on-cycle link in I_i, and q^i_{vu} indicates whether link (v,u) desires to be protected by I_i. For an on-cycle link (v,u), the length of the corresponding protection path is $D_{\mathrm{vu}} = \sum_{(v,u)\in E} d_{\mathrm{vu}} \cdot x^i_{\mathrm{vu}} - d_{\mathrm{vu}}$, while for a straddling link

(v,u), the lengths of the two protection paths are $D^1_{\mathrm{vu}} = d_{\mathrm{vu}_1} + d_{u_1u_2} + \cdots + d_{u_nu}$ and $D^2_{\mathrm{vu}} = d_{\mathrm{vv}_1} + d_{v_1v_2} + \cdots + d_{v_nu}$, respectively. The line rate assignment constraint depends on the lengths of protection paths for different types of links.

1) *Link* (v,u) *with* $q^i_{\mathrm{vu}} = 1$.
   a) *On-cycle link* (v,u) *with* $q^i_{\mathrm{vu}} = 1$: Then length of protection path for link (v,u) should be smaller than $h_{\max}$, i.e., $D_{\mathrm{vu}} = \sum_{(v,u)\in E} d_{\mathrm{vu}} \cdot x^i_{\mathrm{vu}} - d_{\mathrm{vu}} \le h_{\max}$. The line rate b^i_r for D_{vu} is restricted by the following constraint:
   $$\frac{\sum_{a\in E} d_a \cdot x^i_a - d_{\mathrm{vu}}}{h_r} \le \frac{h_{\max}}{h_{\min}} \cdot (1 - b^i_r) + b^i_r. \tag{21}$$
   b) *Straddling link* (v,u) *with* $q^i_{\mathrm{vu}} = 1$. Based on the triangle inequality, it is obvious that $d_{\mathrm{vu}} \le D^1_{\mathrm{vu}}$, $d_{\mathrm{vu}} \le D^2_{\mathrm{vu}}$. Thus, the line rate r for D^1_{vu} and D^2_{vu} also can be restricted by constraint (21).
2) *Link* (v,u) *with* $q^i_{\mathrm{vu}} = 0$: In this case, we need to guarantee that the line rate previously assigned still works. In other words, whatever the value of b^i_r, the following constraint (22) is always held, which is derived from constraint (20) by restituting $q^i_{\mathrm{vu}} = 0$
   $$\frac{\sum_{a\in E} d_a \cdot x^i_a}{h_r} \le \frac{h_{\max}}{h_{\min}} \cdot (1 - b^i_r) + b^i_r + \frac{d_{\max}}{h_r}. \tag{22}$$
   Let $d_{\max}$ indicate the longest links in a network topology, then the longest p-cycle circumference will be $(h_{\max} + d_{\max})$, thus for any p-cycle, $\sum_{a\in E} d_a \cdot x^i_a \le h_{\max} + d_{\max}$. When $b^i_r = 0$, constraint (22) is held. When $b^i_r = 1$, it means that there exits a least a link b desiring to be protected by I_i, no matter it is on-cycle link or straddling link, we can get from Theorem 1 that $\sum_{a\in E} d_a \cdot x^i_a - d_b \le h_r$. Since $d_b \le d_{\max}$, we have $\sum_{a\in E} d_a \cdot x^i_a \le h_r + d_{\max}$. As a result, we can see that constraint (22) is always satisfied for the case $q^i_{\mathrm{vu}} = 0$ whatever the value of b^i_r, and the line rate previously assigned (restricted by the links with $q^i_{\mathrm{vu}} = 1$) still works.

Thus, the path-length-limited p-cycle can be found with constraint (20) as well as its proper line rate. ■

Considering all the situations that whether the link (v,u) has the desire q^i_{vu} to be protected by I_i, appropriate line rate is assigned for I_i with the constraint (20). This constraint will overcomes the shortcomings of extra CAPEX cost and infeasible solution in constraint (7). We use the novel constraint (20) to replace constraint (7) in the p-cycle design MILP model.

D. Discussion

The proposed MILP model enables to guarantee the optimal p-cycle design in transparent optical networks. Meanwhile, our MILP model can be easily extended to translucent or opaque optical networks with O/E/O regenerators [34]. In these optical networks, the introduction of O/E/O regenerators extends transmission reach and enables more flexible line rate assignments. However, the regenerators also add CAPEX cost. Thus, both extended transmission reach and added CAPEX cost need to be taken into account. These considerations can be formulated by adding two variables g_v and g^i_v, where g_v indicates whether a regenerator needs to be placed in node v and g^i_v indicates whether p-cycle I_i uses the regenerator in node v, respectively. Only objective function in equation (1) and line rate assignment constraint (20) need to be modified as follows:

$$\min \quad \beta \cdot C_T + \theta \cdot C_L + \gamma \cdot C_R \tag{23}$$

$$C_R = \sum_{v\in V} e \cdot g_v \tag{24}$$

where e is the cost of one O/E/O regenerator, and γ is an adjustable parameters for weighting of C_R

$$\frac{\sum_{a\in E} d_a \cdot x^i_a - q^i_{\mathrm{vu}} \cdot d_{\mathrm{vu}} - \sum_{v\in V} g^i_v \cdot D_R}{h_r} \le \frac{h_{\max}}{h_{\min}} \cdot (1 - b^i_r) + b^i_r + \frac{d_{\max}}{h_r} \cdot (1 - q^i_{\mathrm{vu}}) \qquad \forall i, \forall r, \forall v, \forall u, u > v \tag{25}$$

$$g^i_v \le y^i_v, \quad \forall i, \forall v \tag{26}$$

$$g_v \ge g^i_v, \quad \forall i, \forall v. \tag{27}$$

Here, we consider the impact of regenerators by introducing a constant extended distance D_R, then line rate assignment can be achieved by constraints (25)–(27). Moreover, these constraints involve regenerator placement problem, which has been considered as a high complexity problem [35].

V. Time-Efficient Algorithms For MILP Model

In this section, we develop two algorithms to solve the MILP model time-efficiently. Even though the proposed model manages to obtain the optimal solution in small network topologies, as the network size increases, it takes a long time to get the optimal solution. To increase the scalability, GPA algorithm is designed to partition the network topology into small sub-graphs in average, then the optimal p-cycles can be obtained in different sub-graphs in parallel. We further observe that the number of required p-cycles (i.e., $|I|$) in the MILP model largely affects computing time, and design Estimation of $|I|$ (EI) algorithm to estimate the enough number of required p-cycles.

A. GPA Algorithm

Inspired by the graph partitioning method for multi-domain optical networks in [10], we propose a GPA algorithm based on spectral clustering [36] to perform concurrent computation in p-cycle design for MLR optical networks.

In GPA algorithm, we first compute the Laplacian matrix $L = D - W$ for network $G(V,E)$, and obtain its eigenvalues and eigenvectors. Then, according to the number of sub-graphs (say k), we choose k eigenvectors corresponding to the k smallest eigenvalues, and apply k-means algorithm [36] to minimize the number of inter-links connecting different sub-graphs. We also use k-means algorithm to guarantee that the sub-graphs have as equal number of intra-links as possible, which is efficient for concurrent computation. Regarding the inter-links, we distribute them averagely to be protected by different sub-graphs. In each sub-graph, p-cycles are generated using MILP model in

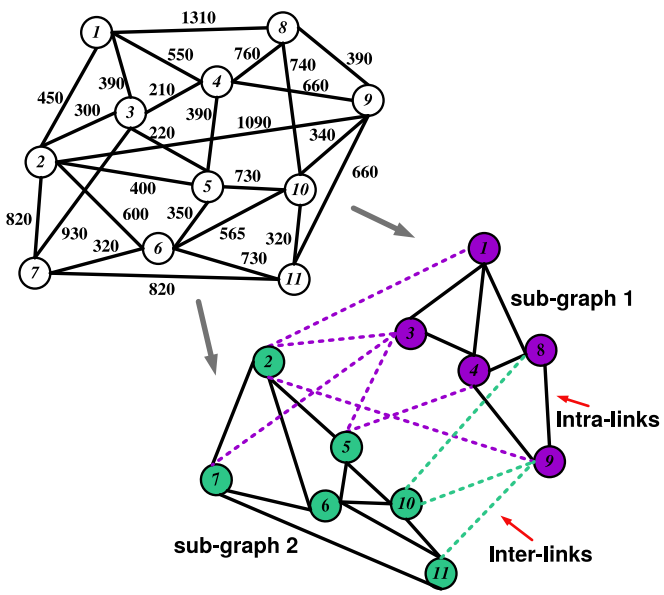

Fig. 6. European COST239 Network [7] with two sub-graphs partitioning.

Section IV-A based on intra-links, inter-links to other sub-graphs, and the links connecting the nodes of inter-links in other sub-graphs. However, for a specific sub-graph, not all the links need to be protected, only intra-links in the p-cycle and partial inter-links are required to be protected.

Algorithm 1: Graph Partitioning in Average Algorithm.

Input: Network topology $G(V, E)$ and traffic matrix
Output: The optimal p-cycles
1: calculate matrix W and D in $G(V, E)$, where W is the adjacency matrix of G and D is an $n \times n$ diagonal matrix composed of the degree of each node in G;
2: compute the Laplacian matrix $L = D - W$;
3: compute the eigenvalues and eigenvectors of L;
4: k=1;
5: **for** $k = k + 1$ **do**
6: **if** $k \leq 4$ **then**
7: choose k eigenvectors of L corresponding to the smallest k eigenvalues;
8: partition $G(V, E)$ into sub-graphs in average using k-means algorithm [36];
9: distribute inter-links to be protected among these sub-graphs in average;
10: solve the MILP model in Section IV-A for sub-graphs in parallel;
11: obtain the optimal p-cycles;
12: **end if**
13: **end for**

We give an example to illustrate the GPA algorithm with two sub-graphs partitioning in European COST239 network in Fig. 6. In sub-graph-1, p-cycles are generated based on intra-links in sub-graph-1, inter-links (i.e., (1,2), (3,2), (3,5), (3,7), (4,5), (8,10), (9,10), (9,2) and (9,11)), and links connecting the nodes of inter-links in sub-graph-2 (i.e., links (2,5), (2,7), (5,10), (7,11) and (10,11)). However, only partial inter-links (1,2), (3,2), (3,5), (3,7), (4,5) and (9,2) are chosen to be protected by p-cycles in sub-graph-1 so that sub-graph-1 and sub-graph-2 have the same number of working links (13 links). The p-cycles in sub-graph-2 are obtained using the same method.

B. EI Algorithm

The value of $|I|$ should be sufficiently large to ensure that the proposed MILP model manages to obtain optimal solution. However, a larger $|I|$ will slow down the computing time. In [15], $|I|$ is estimated by tending to straddle the heaviest load links whose incident nodes have degrees larger than 2. But this method is not valid in our model, since they do not consider different protection capacity provided by different line rates in the p-cycles.

Algorithm 2: Estimation of $|I|$ Algorithm.

Input: Traffic matrix, transponder cost t_r at line rate $r \in R$
Output: The number $|I|$ of p-cycles required in MILP model
1: **for** each link $(v, u) \in E$ with traffic load l_{vu} **do**
2: choose the p-cycles with cost-effective transponders to protect the traffic load l_{vu};
3: calculate the total number of required p-cycles at 100 Gb/s with equation (28);
4: calculate the total number of required p-cycles at 40 Gb/s with equation (29);
5: calculate the total number of required p-cycles at 10 Gb/s with equation (30);
6: sum the total number of p-cycles for protecting traffic loads l_{vu};
7: **end for**
8: obtain the total number of required p-cycles for protecting all the traffic load with (31);

In EI algorithm, we estimate the number of p-cycles $|I|$ required in MILP model according to traffic loads and transponder cost. For each link in $G(V, E)$, we choose the p-cycles with minimum transponder cost to protect the traffic load. Table II explains how to choose such p-cycles for protecting traffic load below 100 Gb/s. Note that the method can be simply applied for larger traffic load. We summarize the following Equations (28)–(30) to calculate the total number of required p-cycles to protect traffic load l_{vu} on link (v, u) at 10, 40 and 100 Gb/s line rates, respectively

$$C_{100} = \lfloor \frac{l_{\mathrm{vu}} + 49}{100} \rfloor \tag{28}$$

$$C_{40} = \lfloor \frac{\max\{19 + l_{\mathrm{vu}} - C_{100} \cdot 100, 0\}}{40} \rfloor \tag{29}$$

$$C_{10} = \lceil \frac{\max\{9 + l_{\mathrm{vu}} - C_{100} \cdot 100 - C_{40} \cdot 40, 0\}}{10} \rceil. \tag{30}$$

TABLE II
METHOD FOR CHOOSING COST-EFFECTIVE p-CYCLES

Traffic $l_{vu}(Gbps)$	$[1, 10]$	$[11, 20]$	$[21, 40]$	$[41, 50]$	$[51, 100]$
Required p-cycle	⊕	⊕⊕	⊙	⊕⊙	⊗
Optimal cost t_r	1	2	2.5	3.5	3.75

⊕ 10 *Gbps* p-cycle ⊙ 40 *Gbps* p-cycle ⊗ 100 *Gbps* p-cycle

Then, the total number of p-cycles $|I|$ is obtained by equation (31). Because there exists at least three links in one p-cycle and a small positive integer δ is added in case that $|I|$ is not large enough

$$|I| = \delta + \frac{1}{3} \sum_{(v,u)\in E} (C_{100} + C_{40} + C_{10}) . \tag{31}$$

VI. PERFORMANCE EVALUATIONS

We use CPLEX 12.06 to solve the proposed MILP model on an Intel Core PC equipped with a 3.5 GHz CPU and 8 GB RAM. Three networks are used as test beds: European COST239 (11 *nodes*, 52 *directed links*, and *average nodal degree* 4.7 in Fig. 6 [5], NSFNET (14 *nodes*, 44 *directed links* and *average nodal degree* 3.1) [3] and US Backbone networks (28 *nodes*, 90 *directed links* and *average nodal degree* 3.2) [3]. In order to guarantee there exists at least one protection path ($\leq$ 1800 km) for each link, the link lengths in NSFNET and US Backbone networks are divided by 3 and 2, respectively.

We first evaluate the proposed algorithms for our p-cycle design MILP model in COST239, NSFNET and US Backbone networks. GPA algorithm partitions COST239, NSFNET and US Backbone networks into two sub-graphs, three sub-graphs and four sub-graphs scenarios, respectively. EI algorithm estimates enough number of required p-cycles in each sub-graph. Thereafter, we compare our method with p-cycle design without cycle enumeration in SLR optical networks [15] and p-cycle design with cycle enumeration in MLR optical networks [17].

A. The Efficiency of GPA and EI

We first verify the efficiency of GPA and EI algorithms in COST239 network by solving the MILP model in four cases, i.e., No GPA or EI, EI, GPA and EI+GPA. Due to the computational complexity, we use a server with 500 GB RAM for the cases of No GPA or EI, and EI. For the other cases, only the PC with 8 GB RAM is used. Traffic loads are generated to let maximum link traffic load about 10, 30, 50 and 100 Gb/s after Dijkstra's shortest-path routing, respectively.

The results are shown in Table III. We observe that when neither GPA nor EI is used, the computing time increases dramatically as traffic increases. For the traffic large than 30 Gb/s, even feasible solution cannot be achieved after it exceeds the memory with computing time more than 70 000 s. However, EI algorithm largely reduces computing time and achieves comparable solution compared with the optimal solution in case of No GPA or EI, but it still requires a long computing time for large traffic. Note that the solution 62 for the case of No GPA or EI is even worse because it is obtained with a relative gap 33.11% to the lower bound in CPLEX, and this value does not decrease from computing time 709.42 s to 71809.43 s. GPA algorithm can achieve sub-optimal solution and reduce computing time for larger traffic. Moreover, in more sub-graphs scenario, larger computing time reduction and bigger optimality gap are observed. Finally, we see that using both GPA and EI algorithm further reduces computing time and does not affect the quality of solution.

We can conclude that it is the GPA algorithm that mainly reduces computing time at the expense of introduced optimality gap, however, with both EI and GPA, more computing time reduction can be achieved.

B. p-Cycle Design With GPA and EI

Then, we perform simulations with both GPA and EI algorithms in COST239, NSFNET, US Backbone networks, respectively. Maximum link traffic loads are about 50, 100, 150 and 200 Gb/s, respectively. The results are shown in Table IV and Fig. 7. The following two metrics are used to evaluate the performance of p-cycles in different sub-graphs scenarios:

1) *CAPEX Cost*: CAPEX cost is evaluated as total protection cost of p-cycles generated by the MILP model.
2) *Computing Time*: Computing time is used to evaluate the GPA and EI algorithms.

In COST239 network, we can see that the CAPEX cost in Fig. 7(a) increases with the number of sub-graphs, while the computing time in Table IV is greatly reduced. Specifically, at low traffic, the CAPEX cost in four sub-graphs scenario is approximately 17% and 17% bigger at 50 Gb/s traffic and 11% and 12% bigger at 100 Gb/s traffic in comparison to two sub-graphs scenario and three sub-graphs scenario, respectively. Whereas, the computing time in these sub-graphs scenarios does not differ too much. As the traffic increases, the computing time in two sub-graphs scenario is 10446.41 s (nearly 3 h) at 150 Gb/s traffic, and 53961.45 s (nearly 15 h) at 200 Gb/s traffic, however, four sub-graphs scenario largely decreases the computing time to only 109.13 s at 150 Gb/s traffic and 29.16 s at 200 Gb/s traffic with the low CAPEX cost expense, which are 16% and 28% bigger than that in two sub-graphs scenario, respectively.

In NSFNET network, it shows some differences from COST239 network. As we can see from Fig. 7(b) and Table IV, three sub-graphs scenario achieves the lowest CAPEX cost and also the smallest computing time. Specifically, at the traffic 50, 100, 150 and 200 Gb/s, the CAPEX cost in three sub-graphs scenario is 5% and 2%, 8% and 9%, 6% and 11%, 5% and 2% smaller than that in two sub-graphs scenario and four sub-graphs scenario, respectively. Compared with the computing time about 31676.07 s(nearly 8 h) at traffic 200 Gb/s in two sub-graphs scenario, it is only 100.78 s in three sub-graphs scenario.

To show the scalability of our method, we also show the p-cycle results in US Backbone network in Fig. 7(c) and Table IV. It is worth noting that differences of CAPEX cost in various sub-graphs are quite small (less than 8%). The four sub-graphs scenario even spends smaller CAPEX cost than two sub-graphs

TABLE III
COMPUTING TIME AND OPTIMALITY GAP WITH DIFFERENT APPROACHES (NO EI OR GPA, EI, GPA AND GPA+EI) IN COST239 NETWORK

Traffic		No EI or GPA	EI	GPA			GPA+EI		
		1 graph	1 graph	2 sub-graphs	3 sub-graphs	4 sub-graphs	2 sub-graphs	3 sub-graphs	4 sub-graphs
10 Gb/s	Objective	38.5	38.5	49	63	75	49	63	75
	Time	421.38 s	169.43 s	24.43 s	6.24 s	2.12 s	1.34 s	1.35 s	0.33 s
	Gap *	–	0%	21.4%	38.8%	48.6%	21.4%	38.8%	48.6%
30 Gb/s	Objective	62	58	63	67	80.5	63	67	80.5
	Time	71809.43 s	26124.48 s	54.14 s	10.78 s	23.75 s	2.62 s	2.13 s	0.63 s
	Gap *	–	0%	7.9%	13.4%	27.9%	7.9%	13.4%	27.9%
50 Gb/s	Objective	–	76.5	80	80	94	80	80	94
	Time	79045.77 s	39468.50 s	6325.95 s	38.94 s	7.92 s	4.12 s	3 s	0.12 s
	Gap *	–	0%	4.4%	4.4%	18.6%	4.4%	4.4%	18.6%
100 Gb/s	Objective	–	108	115.5	114	128.75	115.5	114	128.75
	Time	76213.17 s	46343.75 s	27135.7 s	7143.32 s	409.56 s	633.01 s	11.42 s	0.69 s
	Gap *	-	0%	6.5%	5.3%	16.2%	6.5%	5.3%	16.2%

- Feasible solution cannot be obtained after exhausting all the memory. * Gap means the optimality gap to the solution with only EI. algorithm.

TABLE IV
COMPUTING TIME IN DIFFERENT SUB-GRAPHS SCENARIOS IN COST239, NSFNET AND US BACKBONE NETWORKS

Traffic	COST239			NSFNET			US Backbone		
	2 sub-graphs	3 sub-graphs	4 sub-graphs	2 sub-graphs	3 sub-graphs	4 sub-graphs	2 sub-graphs	3 sub-graphs	4 sub-graphs
50 Gb/s	4.12 s	3 s	0.12 s	4.52 s	3.02 s	0.56 s	9523.91 s	20.14 s	0.56 s
100 Gb/s	633.01 s	11.42 s	0.69 s	463.17 s	8.85 s	2.03 s	12635.45 s	5681.74 s	3.64 s
150 Gb/s	10446.41 s	507.12 s	109.13 s	7426.19 s	59.78 s	4.42 s	34786.53 s	13785.17 s	75.36 s
200 Gb/s	53961.45 s	5218.17 s	29.16 s	31676.07 s	100.78 s	253.34 s	57841.06 s	34561.04 s	1252.27 s

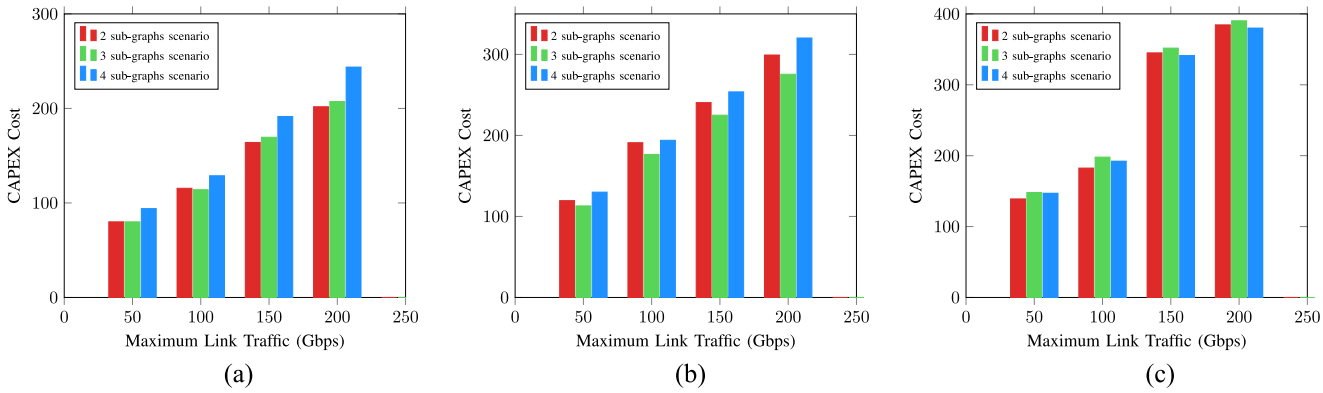

Fig. 7. CAPEX cost of p-cycles in different sub-graphs scenarios in COST239, NSFNET and US Backbone networks. (a) p-Cycle results in COST239 network. (b) p-Cycle results in NSFNET network. (c) p-Cycle results in US Backbone network.

scenario and three sub-graphs scenario as we set a gap at high traffic (10% for two sub-graphs scenario and 5% for three sub-graphs scenario) in CPLEX to ensure the feasible solution with limited memory. Meanwhile, since the US Backbone network has big node set and link set, it takes a long time to generate p-cycles in two sub-graphs scenario, whereas the computing time in four sub-graphs scenario is largely reduced.

The p-cycle results on these three networks indicate that the proposed MILP model is efficiently solved with the help of GPA and EI algorithms, which permit to largely reduce computing time. p-Cycles are generated in the balance between CAPEX cost and computing time in four sub-graphs scenario in COST239 and US Backbone networks, three sub-graphs scenario in NSFNET network.

C. Comparison to SLR-NCE-40 and MLR-CE

The p-cycle results in Section VI-B show that our p-cycle design MILP model is efficient to achieve relatively low cost and low computing time with GPA and EI algorithms. In this section, we further compare our p-cycle results with p-cycle design without cycle enumeration in SLR optical networks in [15], and p-cycle design with cycle enumeration in MLR optical networks in [17]. For the sake of readability, we call the p-cycle

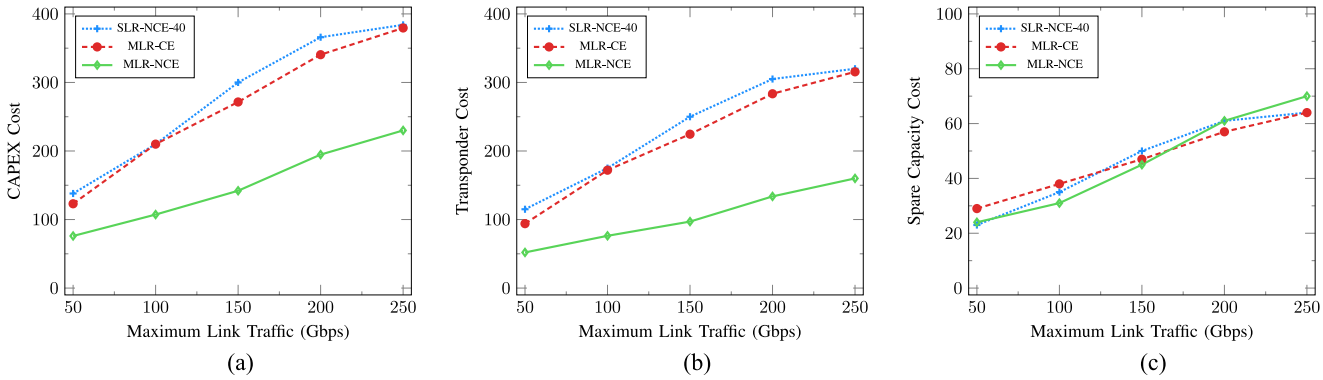

Fig. 8. Protection cost comparison among SLR-NCE-40, MLR-CE and MLR-NCE in COST239 Network. (a) CAPEX cost. (b) Transponder cost. (c) Spare capacity cost.

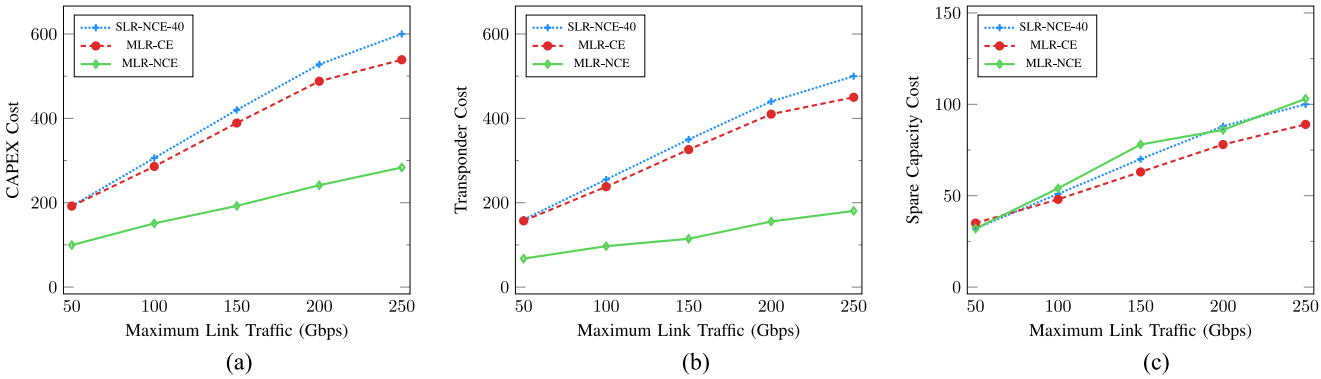

Fig. 9. Protection cost comparison among SLR-NCE-40, MLR-CE and MLR-NCE in NSF Network. (a) CAPEX cost. (b) Transponder cost. (c) Spare capacity cost.

design in [15] as SLR-NCE-40, the p-cycle design in [17] as MLR-CE and our p-cycle design as MLR-NCE.

To conduct the comparison, we use the results of MLR-NCE in 4 sub-graphs scenario in COST239 and US Backbone networks, and three sub-graphs scenario in NSFNET network. In SLR-NCE-40, only 40 Gb/s line rate is assigned as either 10 or 100 Gb/s line rate for p-cycles will increase CAPEX cost. In order to make a fair comparison, we add the transmission reach limits on p-cycles with cycle-circumference-limited constraints in SLR-NCE-40 and MLR-CE. Thus, we have to remove the traffic in some links in the networks as SLR-NCE-40 and MLR-CE are not able to protect all the traffic with such transmission reach limits, which we discuss in Section IV-C. It should be noted that our path-length-limited p-cycles in MLR-NCE enables to protect all the traffic in these networks. The traffic in the following links are removed: $1-8$, $2-9$, $4-8$, $4-9$ and $7-11$ in COST239 network, $1-8$, $4-11$ and $6-14$ in NSFNET network, $8-13$ in US Backbone network. The performance of SLR-NCE-40, MLR-CE and MLR-NCE are evaluated with the following metrics:

1) *CAPEX Cost*: CAPEX cost is the total protection cost for p-cycle design. It consists of transponder cost and spare capacity cost, both of which are weighted 1 in this study.
2) *Transponder Cost*: Transponder cost is the main protection cost in CAPEX Cost.
3) *Number of Transponders*: In MLR-CE and MLR-NCE, transponders are set at $10/40/100$ Gb/s line rates, while in SLR-NCE-40, only 40 Gb/s line rate is assigned. It is valuable to investigate the number of transponders used at each line rate.
4) *Spare Capacity Cost*: Spare capacity is pre-configured on each link in p-cycles for potential failures. It is also a significant metric for CAPEX cost.

We observe that MLR-NCE achieves significantly lower CAPEX cost in comparison to SLR-NCE-40 and MLR-CE in all the network instances in Figs. 8(a), 9(a), 10(a). Specifically, compared with SLR-NCE-40 that generates p-cycles at 40 Gb/s without cycle enumeration, MLR-NCE achieves CAPEX cost savings about 46.68% in average in COST239 network, 52.00% in average in NSFNET network and 53.18% in average in US Backbone network. The valuable CAPEX cost reduction comes from the optimal line rate assignment in MLR-NCE for MLR optical networks. Meanwhile, compared with MLR-CE that generates p-cycles at $10/40/100$ Gb/s with cycle enumeration, the average CAPEX cost savings in MLR-NCE are 43.40% in COST239 network, 48.76% in NSFNET network and 46.70% in US Backbone network. It indicates that more CAPEX cost in MLR-NCE is reduced compared with SLR-NCE-40, this is because that SLR-NCE-40 uses only 40 Gb/s line rate for all the p-cycles.

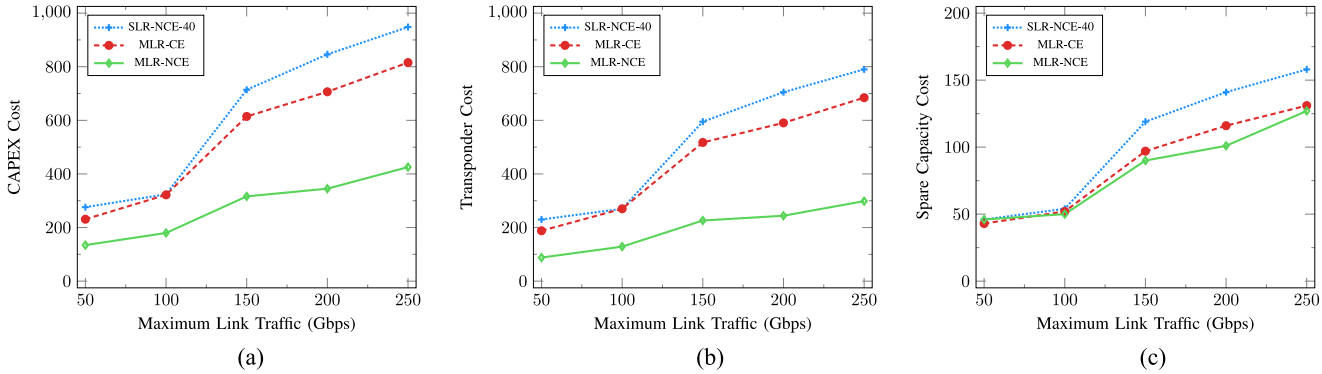

Fig. 10. Protection cost comparison among SLR-NCE-40, MLR-CE and MLR-NCE in US Backbone Network. (a) CAPEX cost. (b) Transponder cost. (c) Spare capacity cost.

TABLE V
NUMBER OF TRANSPONDERS USED AT EACH LINE RATE IN SLR-NCE-40, MLR-CE AND MLR-NCE

Traffic		COST239			NSFNET			US Backbone		
		SLR-NCE-40	MLR-CE	MLR-NCE	SLR-NCE-40	MLR-CE	MLR-NCE	SLR-NCE-40	MLR-CE	MLR-NCE
50 *Gbps*	⊕	—	34	2	—	12	0	—	18	16
	⊙	46	24	20	64	58	27	92	68	29
	⊗	—	0	0	—	0	0	—	0	0
	Total	46	58	22	64	70	27	92	86	45
100 *Gbps*	⊕	—	12	0	—	8	2	—	0	0
	⊙	70	64	26	102	80	38	108	96	47
	⊗	—	0	3	—	8	0	—	8	3
	Total	70	76	29	102	96	40	108	104	50
150 *Gbps*	⊕	—	12	2	—	6	12	—	10	0
	⊙	100	76	35	140	104	35	238	146	71
	⊗	—	6	2	—	16	4	—	38	25
	Total	100	94	39	140	126	51	238	194	96
200 *Gbps*	⊕	—	6	10	—	0	3	—	38	4
	⊙	121	102	42	176	140	55	282	140	54
	⊗	—	6	5	—	16	4	—	54	28
	Total	121	114	57	176	156	62	282	232	86
250 *Gbps*	⊕	—	8	11	—	10	8	—	32	11
	⊙	128	114	44	200	152	63	316	168	67
	⊗	—	6	6	—	16	4	—	62	32
	Total	128	128	61	200	178	75	316	262	110

⊕ 10 *Gbps p*-cycle ⊙ 40 *Gbps p*-cycle ⊗ 100 *Gbps p*-cycle

Next, we conduct clear presentation of transponder cost and spare capacity cost of the CAPEX cost in these three network instances. From Figs. 8(b), (c), 9(b), (c), 10(b), (c), we can see that the transponder cost in MLR-NCE is much lower than in SLR-NCE-40 and MLR-CE, while the spare capacity cost does not show many differences. Specifically, comparing with SLR-NCE-40, MLR-NCE achieves average transponder cost savings about 55.71% in COST239 network, 63.12% in NSFNET network and 60.73% in US Backbone network, while, in comparison to MLR-CE, the average transponder cost savings in MLR-NCE is 51.85% in COST239 network, 60.62% in NSFNET network and 55.37% in US Backbone network. The spare capacity cost in MLR-NCE is reduced less than transponder cost. In comparison to SLR-NCE-40, the spare capacity cost savings are 1.54% and 15.95% in average in COST239 network and in US Backbone network, respectively. While compared with MLR-CE, the spare capacity cost savings are 4.71% and 4.01% in average in COST239 network and in US Backbone network, respectively. However, in NSFNET network, the spare capacity cost in MLR-NCE is even 3.61% and 10.74% bigger than in SLR-NCE-40 and MLR-CE, respectively. This is because that the inter-links among sub-graphs in MLR-NCE may be used several times, thus it requires more spare capacity.

It can be concluded that transponder cost savings mainly contributes to the reduction of CAPEX cost in MLR-NCE. As the transponders used in MLR-CE and MLR-NCE distribute in

various line rates, then we make a deeper insight into the number of transponders used at various line rates in Table V. We observe that SLR-NCE-40 uses the biggest number of transponders for p-cycle protection as only 40 Gb/s line rate is assigned. Even though the p-cycles in MLR-CE and MLR-NCE are able to be assigned $10/40/100$ Gb/s, most of the transponders are set at 40 Gb/s line rate, this is because 40 Gb/s line rate for p-cycle reaches a compromise between the transmission reach and transponder cost. However, in MLR-NCE, fewer than half of the transponders in SLR-NCE-40 and MLR-CE are used. There are several reasons for the reduction. First of all, just enough transponders are laid for each p-cycle in MLR-NCE. Specifically, unlike the layout of transponders in SLR-NCE-40 or MLR-CE, in which one pair of transponders are laid on each protection path, only one transponder is laid on the node that incident to the protection path in MLR-NCE. Thus, it will reduce the number of transponders. Moreover, path-length-limited p-cycles are generated in MLR-NCE, while SLR-NCE-40 and MLR-CE generate the cycle-circumference-limited p-cycles, which bring extra protection cost, as discussed in Section IV-C. In addition, MLR-NCE offers a way to directly generate the optimal p-cycles in MILP model without candidate cycle enumeration.

The comparison results demonstrate that our p-cycle design MLR-NCE achieves significant CAPEX cost savings (more than 40%) in comparison to SLR-NCE-40 and MLR-CE. The main cost savings comes from the transponder cost, which is further optimized in our path-length-limited p-cycles. Moreover, the p-cycle design MILP model manages to obtain the optimal solution which uses exactly the minimum CAPEX cost in p-cycle protection for MLR optical networks.

VII. Conclusion

We investigate distance-adaptive p-cycle design for MLR optical networks. Based on path-length-limited p-cycles with transmission reach limits on each protection path, we propose an MILP model to directly generate optimal p-cycles with the minimum CAPEX cost instead of candidate cycle enumeration. We also develop GPA algorithm and EI algorithm to make the proposed MILP model scalable, which are proved to largely reduce computing time. Extensive simulations demonstrate that our proposed p-cycle design achieves significant CAPEX cost savings for MLR optical networks, especially the transponder cost savings, in comparison to p-cycle design with SLR and p-cycle design with candidate cycle enumeration.

References

[1] X. Liu, L. Gong, and Z. Zhu, "Design integrated RSA for multicast in elastic optical networks with a layered approach," in *Proc. IEEE Global Commun. Conf.*, Dec. 2013, pp. 2346–2351.

[2] W. Lu, Z. Zhu, and B. Mukherjee, "On hybrid IR and AR service provisioning in elastic optical networks," *J. Lightw. Technol.*, vol. 33, no. 22, pp. 4659–4670, Nov. 2015.

[3] L. Gong, X. Zhou, X. Liu, W. Zhao, W. Lu, and Z. Zhu, "Efficient resource allocation for all-optical multicasting over spectrum-sliced elastic optical networks," *J. Opt. Commun. Netw.*, vol. 5, no. 8, pp. 836–847, Aug. 2013.

[4] A. Klekamp and U. Gebhard, "Performance of elastic and mixed-line-rate scenarios for a real IP over DWDM network with more than 1000 nodes [invited]," *J. Opt. Commun. Netw.*, vol. 5, no. 10, pp. A28–A36, Oct. 2013.

[5] P. Chowdhury, M. Tornatore, A. Nag, E. Ip, T. Wang, and B. Mukherjee, "On the design of energy-efficient mixed-line-rate MLR optical networks," *J. Lightw. Technol.*, vol. 30, no. 1, pp. 130–139, Jan. 2012.

[6] M. Liu, M. Tornatore, and B. Mukherjee, "New strategies for connection protection in Mixed-Line-Rate optical WDM networks," *J. Opt. Commun. Netw.*, vol. 3, no. 9, pp. 641–650, Sep. 2011.

[7] F. Zhou, "Multicast provision in transparent optical networks with mixed line rates," in *Proc. Opt. Netw. Des. Model. Conf.*, Apr. 2013, pp. 125–130.

[8] J.-X. Cai, C. Davidson, A. Lucero, H. Zhang, D. Foursa, O. Sinkin, W. Patterson, A. Pilipetskii, G. Mohs, and N. S. Bergano, "20 tbit/s transmission over 6860 km with sub-nyquist channel spacing," *J. Lightw. Technol.*, vol. 30, no. 4, pp. 651–657, Feb. 2012.

[9] F. Zhang and W.-D. Zhong, "Applying p-cycles in dynamic provisioning of survivable multicast sessions in optical WDM networks," in *Proc. Opt. Fiber Commun. Conf.*, Anaheim, CA, USA, Mar. 2007, Paper JWA74.

[10] H. Drid, B. Cousin, M. Molnar, and S. Lahoud, "A survey of survivability in multi-domain optical networks," *Comput. Commun.*, vol. 33, no. 8, pp. 1005–1012, May 2010.

[11] P. K. Agarwal, A. Efrat, S. Ganjugunte, D. Hay, S. Sankararaman, and G. Zussman, "The resilience of WDM networks to probabilistic geographical failures," *IEEE/ACM Trans. Netw.*, vol. 21, no. 5, pp. 1525–1538, Oct. 2013.

[12] D. A. Schupke, "An ILP for optimal p-cycle selection without cycle enumeration," presented at the Optical Network Design Modeling Conf., Ghent, Belgium, Feb. 2004.

[13] B. Wu, K. L. Yeung, and P. Ho, "ILP formulations for non-simple p-cycle and p-trail design in WDM mesh networks," *Comput. Netw.*, vol. 54, no. 5, pp. 716–725, Apr. 2010.

[14] W. Grover and D. Stamatelakis, "Cycle-oriented distributed preconfiguration: Ring-like speed with mesh-like capacity for self-planning network restoration," in *Proc. IEEE Int. Conf. Commun.*, Jun. 1998, pp. 537–543.

[15] B. Wu, K. L. Yeung, and P. Ho, "ILP formulations for p-cycle design without candidate cycle enumeration," *IEEE/ACM Trans. Netw.*, vol. 18, no. 1, pp. 284–295, Feb. 2010.

[16] M. Ju, F. Zhou, Z. Zhu, and S. Xiao, "p-Cycle design without candidate cycle enumeration in Mixed-Line-Rate optical networks," in *Proc. Int. Conf. High Perform. Switch. Routing*, Jul. 2015, pp. 1–6.

[17] H. Drid, N. Brochier, E. L. Rouzic, and N. Ghani, "P-cycle design for mixed-line rate optical networks," in *Proc. Opt. Netw. Des. Model. Conf.*, Apr. 2012, pp. 1–4.

[18] M. Liu, M. Tornatore, and B. Mukherjee, "Efficient shared subconnection protection in mixed-line-rate optical WDM networks," *J. Opt. Commun. Netw.*, vol. 5, no. 11, pp. 1227–1235, Nov. 2013.

[19] C. S. Vadrevu, R. Wang, M. Tornatore, C. U. Martel, and B. Mukherjee, "Survivable provisioning in Mixed-Line-Rate networks using multi-path routing," presented at the Optical Fiber Communication Conf., Los Angeles, CA, USA, Mar. 2012, Paper OTh4B.3.

[20] D. A. Schupke, C. G. Gruber, and A. Autenrieth, "Optimal configuration of p-cycles in WDM networks," in *Proc. Int. Conf. Commun.*, Apr. 2002, pp. 2761–2765.

[21] L. Ruan, F. Tang, and C. Liu, "Dynamic establishment of restorable connections using p-cycle protection in WDM networks," *Photon. Netw. Commun.*, vol. 11, no. 3, pp. 301–311, May 2006.

[22] J. Doucette, P. Giese, and W. Grover, "Combined node and span protection strategies with node-encircling p-cycles," in *Proc. Des. Rel. Commun. Netw. Workshops*, Oct. 2005, pp. 213–221.

[23] J. Akpuh and J. Doucette, "Enhanced failure-specific p-cycle network dual-failure restorability design and optimization," *J. Opt. Netw.*, vol. 8, no. 1, pp. 1–13, Jan. 2009.

[24] P. Cholda and A. Jajszczyk, "Reliability assessment of p-cycles," presented at the IEEE Global Communication Conf., St. Louis, MO, USA, Nov. 2005, vol. 1, p. 5.

[25] J. Akpuh and J. Doucette, "Sizing eligible route sets for restorable network design and optimization," in *Proc. IEEE Int. Conf. Commun.*, May. 2008, pp. 5292–5299.

[26] J. Doucette, D. He, W. Grover, and O. Yang, "Algorithmic approaches for efficient enumeration of candidate p-cycles and capacitated p-cycle network design," in *Proc. Des. Rel. Commun. Netw. Workshops*, Oct. 2003, pp. 212–220.

[27] W. D. Grover and J. Doucette, "Advances in optical network design with p-cycles: Joint optimization and pre-selection of candidate p-cycles," in *Proc. Lasers Electro-Opt. Soc.*, Nov. 2002, pp. 49–50.

[28] S. Sebbah and B. Jaumard, "An efficient column generation design method of p-cycle-based protected working capacity envelope," *Photon. Netw. Commun.*, vol. 24, no. 3, pp. 167–176, Dec. 2012.

[29] H. A. Pereira, D. A. R. Chaves, C. J. A. Bastos-Filho, and J. F. Martins-Filho, "OSNR model to consider physical layer impairments in transparent optical networks," *Photon. Netw. Commun.*, vol. 18, no. 2, pp. 137–149, 2008.
[30] R. Asthana and Y. N. Singh, "Distributed protocol for removal of loop backs and optimum allocation of p-cycles to minimize the restored path lengths," *J. Lightw. Technol.*, vol. 26, no. 5, pp. 616–627, Mar. 2008.
[31] R. Yadav, R. Yadav, and H. Singh, "P-cycle based network design to control the optical path lengths in restored state of transparent network," in *Proc. Int. Conf. Comput. Commun. Technol.*, Sep. 2010, pp. 355–359.
[32] A. Kodian, A. Sack, and W. D. Grover, "The threshold hop-limit effect in p-cycles: Comparing hop- and circumference-limited design," *Opt. Switch. Netw.*, vol. 2, no. 2, pp. 72–85, Sep. 2005.
[33] T. Panayiotou, G. Ellinas, and N. Antoniades, "p-cycle-based protection of multicast connections in metropolitan area optical networks with physical layer impairments constraints," *Opt. Switching Netw.*, vol. 19, pp. 66–77, 2015.
[34] Z. Zhu, M. Funabashi, Z. Pan, B. Xiang, L. Paraschis, and S. Yoo, "Jitter and amplitude noise accumulations in cascaded all-optical regenerators," *J. Lightw. Technol.*, vol. 26, no. 12, pp. 1640–1652, Jun. 2008.
[35] M. Flammini, A. Marchetti-Spaccamela, G. Monaco, L. Moscardelli, and S. Zaks, "On the complexity of the regenerator placement problem in optical networks," *IEEE/ACM Trans. Netw.*, vol. 19, no. 2, pp. 498–511, Apr. 2011.
[36] U. V. Luxburg, "A tutorial on spectral clustering," *Statist. Comput.*, vol. 17, no. 4, pp. 395–416, Dec. 2007.

Min Ju (S'15) received the B.S. degree from the University of Electronic Science and Technology of China, Chengdu, China, in 2012. She is currently working toward the joint Ph.D. degree from Shanghai Jiao Tong University, Shanghai, China, and the University of Avignon, Avignon, France.

Fen Zhou (SM'15) received the Ph.D. degree in computer science from Institut National des Sciences Appliquées de Rennes, Rennes, France, in 2010. He is currently an Associate Professor at the Computer Science Lab of the University of Avignon, Avignon, France. His research interests include routing optimization and resource allocation in optical networks, content delivery networks, and vehicular networks.

Zuqing Zhu received the Ph.D. degree from the Department of Electrical and Computer Engineering, University of California, Davis, CA, USA, in 2007. From July 2007 to January 2011, he was with the Service Provider Technology Group of Cisco Systems, San Jose, CA, as a Senior Engineer. In January 2011, he joined the University of Science and Technology of China, Hefei, China, where he is currently a Full Professor. He has published more than 150 papers in peer-reviewed journals and conferences. He is an Editorial Board Member of the IEEE COMMUNICATIONS MAGAZINE, *Journal of Optical Switching and Networking* (Elsevier), *Telecommunication Systems Journal* (Springer), *Photonic Network Communications* (Springer), etc. He has also served as a Guest Editor for the IEEE COMMUNICATIONS MAGAZINE AND IEEE NETWORK. He received the Best Paper Awards from IEEE ICC, in 2013, IEEE GLOBECOM, in 2013, IEEE ICNC, in 2014, and IEEE ICC, in 2015. He is a Senior Member of the OSA.

Shilin Xiao received the M.S. degree from the University of Electronic Science and Technology of China, Chengdu, China, in 1988, and the Ph.D. degree from Shanghai Jiao Tong University (SJTU), Shanghai, China, in 2003. From 1988 to 1999, he was with the Guilin Institute of Optical Communications. Since 2000, he has been at the State Key Laboratory of Advanced Optical Communication Systems and Network, SJTU, where he is currently a Professor. His major research interests include optical communications, especially optical switching and passive optical networks. He has published more than 100 papers in technical journals and conferences. He is a Senior Member of the Chinese Institute of Electronics and the Optical Society of China.